International Journal of Multiphase Flow 37 (2011) 76–83

Contents lists available at ScienceDirect

International Journal of Multiphase Flow

journal homepage: www.elsevier.com/locate/ijmulflow

Mass transfer enhancement at deformable droplets due to Marangoni convection

M. Wegener [a,*], A.R. Paschedag [b]

[a] Chemical & Process Engineering, Technische Universität Berlin, Ackerstraße 71-76, D-13355 Berlin, Germany
[b] Beuth University of Applied Sciences Berlin, Luxemburger Str. 10, D-13353 Berlin, Germany

ARTICLE INFO

Article history:
Received 11 March 2010
Received in revised form 9 August 2010
Accepted 16 August 2010
Available online 20 August 2010

Keywords:
Marangoni convection
Mass transfer
Droplet
Liquid/liquid extraction

ABSTRACT

One of the key design parameters in liquid/liquid extraction is the mass transfer coefficient. A complex list of parameters including fluid dynamics, drop size distribution, chemical properties of the involved species, local interfacial instabilities (Marangoni convection) is required in order to determine the transient evolution of the mass transfer coefficient. The influence of Marangoni convection on single drop mass transfer cannot yet be described in an analytical manner, and empirical correlations available in literature fail to predict the mass transfer process. In the present study, experimental investigations on deformable single droplets in the toluene/acetone/water system are presented which shows strong interfacial instabilities. Parameters varied are the drop diameter, the initial solute concentration and the mass transfer direction. Experimental results are compared with the well-known models by Kronig and Brink and Handlos and Baron. The Kronig and Brink model cannot describe Marangoni dominated systems, but comparisons reveal the influence of deformation on the mass transfer enhancement. In contrary, with a slight modification to the Handlos and Baron model, the mean droplet concentration of the transferred component was successfully modelled as a function of Fourier number.

1. Introduction

Solutal Marangoni convection occurs if the interfacial tension varies along the droplet surface due to concentration gradients. The system tends to minimize its surface energy in expanding regions of lower interfacial tension towards regions of higher interfacial tension. The incipient motion of the interface provokes an additional tangential shear stress component on curved surfaces such as droplets or bubbles. As a consequence, a motion of the fluid layers adjacent to the interface is induced (Sternling and Scriven, 1959).

The tangential shear stress condition including the concentration dependent interfacial tension gradient exhibits the strong coupling between velocity and concentration field. As an example, in liquid/liquid extraction processes, droplets of one phase are dispersed in the continuous ambient phase. A solute is transferred from the droplets into the continuous phase (or vice versa, depending on the extraction problem). If the interfacial tension is sensitive enough to the solute concentration, the latter varying over the droplet surface, Marangoni instabilities will appear. The tangential shear stresses provoke random fluid motion on the surface, provided the surface is not contaminated with surfactants which hinder interfacial motion (Agble and Mendes-Tatsis, 2000; Mekasut et al., 1979). These Marangoni induced shear forces reduce the relative velocity (and increase the drag) between droplet and ambient fluid. As a consequence, the drop rise velocity is temporarily reduced (Wegener et al., 2007, 2009b). In addition, complex chaotic flow structures develop inside the droplet, they replace the toroidal flow (known from moving droplet systems without Marangoni convection, see e.g. Clift et al., 1978; Magarvey and Kalejs, 1963; Spells, 1952) and promote radial mixing and thus the mass transfer coefficient. The concentration gradient reduces with time and the Marangoni convection dampens gradually due to ongoing mass transfer. Finally, the inner circulation replaces the chaotic flow structures and the droplet velocity increases.

For larger droplets, instabilities are superposed by shape deformation and oscillation. The deformation is related to interfacial tension or Weber number, respectively (Loth, 2008), and in case of Marangoni convection, the deformation depends on mass transfer. On the other hand, the drag coefficient closely depends on droplet shape, and internal circulation patterns may vary from spherical droplets, so that shape deformation is another key parameter for mass transfer calculations (Al-Hassan et al., 1992).

To date, the mass transfer problem of a single moving droplet with resistance in both phases (conjugated problem) and simultaneous Marangoni convection with all its interactions is not accessible to any analytical description. Numerical simulations of conjugated mass transfer with Marangoni convection in 2D (Mao and Chen, 2004) and 3D (Wegener et al., 2009a) are only available for spherical droplets. To the authors knowledge, there are no

* Corresponding author.
E-mail addresses: mirco.wegener@tu-berlin.de (M. Wegener), anja.paschedag@beuth-hochschule.de (A.R. Paschedag).

0301-9322/$ - see front matter © 2010 Elsevier Ltd. All rights reserved.
doi:10.1016/j.ijmultiphaseflow.2010.08.005

corresponding numerical investigations of droplets with deformable interfaces published up to now.

Established well-known mass transfer models (amongst others, see Table 1, Newman, 1931; Kronig and Brink, 1950; Calderbank and Korchinski, 1956; Handlos and Baron, 1957) only consider the mass transfer resistance inside spherical droplets and are valid for special conditions. The model developed by Newman is applicable for rigid spheres without internal circulation. Kronig and Brink assume internal circulation following the Hadamard streamlines (small Reynolds numbers, i.e. $Re < 1$ and high Peclet numbers, i.e. $Pe \to \infty$). The extraction rate is 2.5 times higher compared to Newman's solution (Kronig and Brink, 1950). The values for B_n and λ_n can be found e.g. in Petera and Weatherley (2001). Calderbank and Korchinski use the concept of an effective diffusion coefficient RD_A. The equation proposed by Kronig and Brink is well represented by their empirical correlation if R is set to 2.25. Handlos and Baron assume that internal mixing can be described by turbulence-like diffusion, i.e. by random radial convection which superimposes internal circulation. In this model, the Peclet number is required, and the terminal velocity of the droplet v_t should be known. λ_n is set to 2.88. Handlos and Baron only retained the first term of their original solution, and the expression in Table 1 is obtained (Olander, 1966). The model has oftentimes been criticised, see e.g. Hubis and Hartland (1986), but nevertheless, the model shows astonishingly good results in many systems (Slater, 1994).

Henschke and Pfennig (1999) follow the idea of Handlos and Baron in their semi-empirical model to describe mass transfer inside a droplet based on diffusion and mass-transfer-induced turbulence. The Fourier number

$$Fo' = \frac{4}{d_P^2}(D_A + \epsilon)t \tag{1}$$

contains the time t, the droplet diameter d_P, the molecular diffusion coefficient D_A, and a turbulent transfer coefficient

$$\epsilon = \frac{v_t d_P}{C_{IP}(1+\mu^*)} \tag{2}$$

with the terminal drop rise velocity v_t, the viscosity ratio μ^* and an instability constant C_{IP} adjustable to experimental data. Newman's solution is obtained if $C_{IP} \to \infty$, for $C_{IP} \to 0$, inner mixing is infinitely fast. Since the model does not account for internal circulation, the authors suggest, if internal circulation occurs and inner turbulence is low, to use other models (e.g. Kronig and Brink) instead.

Fig. 1 shows the relative mean droplet concentration c^* as a function of Fourier number $Fo_d = 4tD_A/d_P^2$. Model predictions are compared with experimental values published by Schulze (2007) and Wegener et al. (2007). Schulze (2007) investigated the mass transfer at water droplets falling in cyclohexanol, the transfer component is acetic acid. In this system, Reynolds number is low and mass transfer resistance is in the droplet only. A comparison with the models by Kronig and Brink and Calderbank and Korchinski shows that the internal problem can be applied to this system. In the toluene/acetone/water system used by Wegener et al. (2007), Marangoni effects play a major role in the mass transfer process. The Handlos and Baron model gives a fairly good first approximation indicating chaotic mixing inside the droplet in the Marangoni dominated system.

An even better approximation is obtained if the Henschke and Pfennig (with $C_{IP} = 3400$) and the Calderbank and Korchinski (with $R = 13$) models are used. This result shows that mass transfer is enhanced by a factor of about five compared to non-Marangoni dominated systems. The strength of Marangoni convection depends on the absolute concentration. The higher the concentration level is, the higher are possible interfacial tension gradients. In Marangoni dominated systems, the relevant inner convection patterns have to be taken into account in order to describe the mass transfer in single droplets reliably.

The presented models are only valid in the spherical droplet regime. For droplets in the oscillating regime, some few correlations were proposed, e.g. Angelo et al. (1966), Rose and Kintner (1966), Yamaguchi et al. (1975). Some authors propose to use the Handlos and Baron model even though inner circulation may be different (Slater, 1994). For deformed or oscillating droplets with simultaneous Marangoni instabilities, no reliable models exist in literature. Al-Hassan et al. (1992) investigated mass transfer in the toluene/acetone/water and the *n*-heptane/acetone/water system in the oscillating regime. Extraction rates for a given column length are given, but no time resolved measurements. Following their results, the droplet interior is completely mixed. Correlation of results was satisfying with a mean deviation of ±23%.

The scope of the present study is to investigate in time resolved measurements the influence of Marangoni convection on the mass transfer at single deformable organic droplets rising in water. Therefore, the ternary standard test system toluene/acetone/water proposed by the European Federation of Chemical Engineering (EFCE) (Misek et al., 1985) has been used. Both mass transfer directions (dispersed to continuous phase and vice versa, $d \to c$ and $c \to d$, respectively), six different initial solute concentrations

Table 1
Models to predict mass transfer in the dispersed phase (spherical droplets, no resistance in the continuous phase). c^* is the related concentration of the transferred solute A in the droplet: $(\bar{c}_A - mc_{Ac\infty})/(c_{Ad0} - mc_{Ac\infty})$, with the mean solute concentration in the droplet $\bar{c}_A$, the distribution coefficient m, the solute concentration in the continuous phase, far away from the droplet $c_{Ac\infty}$, and the initial solute concentration in the droplet c_{Ad0}.

Author(s)	Related concentration	Eq.
Newman (1931)	$c^* = \frac{6}{\pi^2}\sum_{n=1}^{\infty}\frac{1}{n^2}exp\left[-4\frac{(n\pi)^2 D_A t}{d_P^2}\right]$	(3)
Kronig and Brink (1950)	$c^* = \frac{3}{8}\sum_{n=1}^{\infty}B_n^2 exp\left[-64\frac{\lambda_n D_A t}{d_P^2}\right]$	(4)
Calderbank and Korchinski (1956)	$c^* = 1 - \left(1 - exp\left[-R\frac{4\pi^2 D_A t}{d_P^2}\right]\right)^{1/2}$	(5)
Handlos and Baron (1957)	$c^* = exp\left[\frac{-\lambda_n v_t t}{128 d_P(1+\mu^*)}\right]$	(6)
Henschke and Pfennig (1999)	$c^* = \frac{6}{\pi^2}\sum_{n=1}^{\infty}\frac{1}{n^2}exp[-(n\pi)^2 Fo']$	(7)

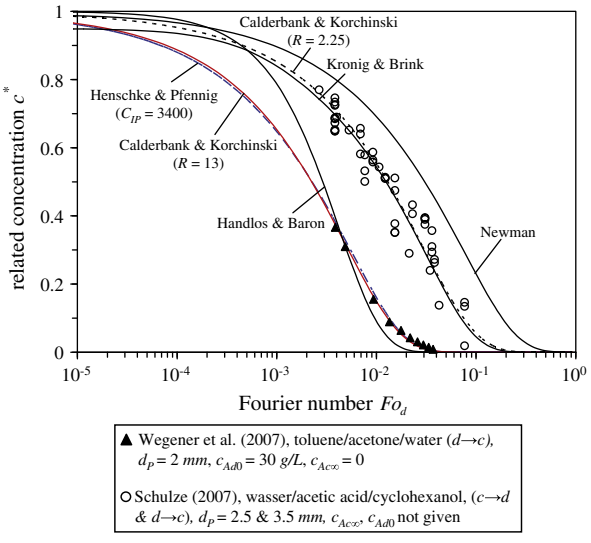

Fig. 1. Related mean droplet concentration c^* as a function of Fourier number $Fo_d = 4tD_A/d_P^2$. Comparisons between model predictions and experimental data from Schulze (2007) and Wegener et al. (2007). Model parameters: $d_P = 2$ mm, $v_t = 100$ mm/s, $C_{IP} = 3400$, $D_A = 2.9 \times 10^{-9}$ m^2/s, $\lambda_n = 2.88$, $\mu^* = 0.62$.

(three for each transfer direction) and diameters up to 6.9 mm have been examined. Special care was taken to keep the system free of contaminants. The obtained results were compared to the models by Kronig and Brink and Handlos and Baron in order to identify the contribution of deformation and Marangoni convection on mass transfer enhancement. Finally, a single parameter is introduced in the Handlos and Baron model to account for the influence of Marangoni convection via the initial solute concentration, reflecting the isotropic nature of the Marangoni induced chaotic flow patterns.

2. Experimental investigations

The experimental setup is shown in Fig. 2. It has been already applied successfully in former mass transfer investigations, see e.g. Wegener et al. (2007). The mass transfer is measured in a glass column (height 1000 mm and inner diameter 75 mm. The inner diameter is large enough to prevent wall influence on fluid motion for all diameters in this study, see as well Wegener et al. (2010)). The column (1) is equipped with a jacket (2) in order to adjust the temperature of the system using a LAUDA thermostat (4) at 25 °C. A precision dosing pump (Hamilton PSD/2 module) (5) generates toluene (6) droplets of desired volume at a nozzle (7). All diameters given in this work correspond to the diameter of a sphere with equivalent volume. Drop release is realised with a solenoid device (8). One glass nozzle and two stainless steel nozzles have been used (N_1: *i.d.* 0.5 mm, N_2: *i.d.* 2 mm and N_3: *i.d.* 3 mm, respectively).

Before each run, the organic and aqueous phase were mutually saturated in a stirred tank (9) to avoid mass transfer between both phases. Due to the sensitivity to impurities of the system, a precise cleaning procedure has been accomplished and only chemicals of high purity have been used: toluene p.a. ⩾99.9% and acetone p.a. ⩾99.8% (both provided by Merck), highly purified deionized water with a specific resistance of 18.3 MΩ cm. The physical properties published by Misek et al. (1985) of the pure components are given in Table 2.

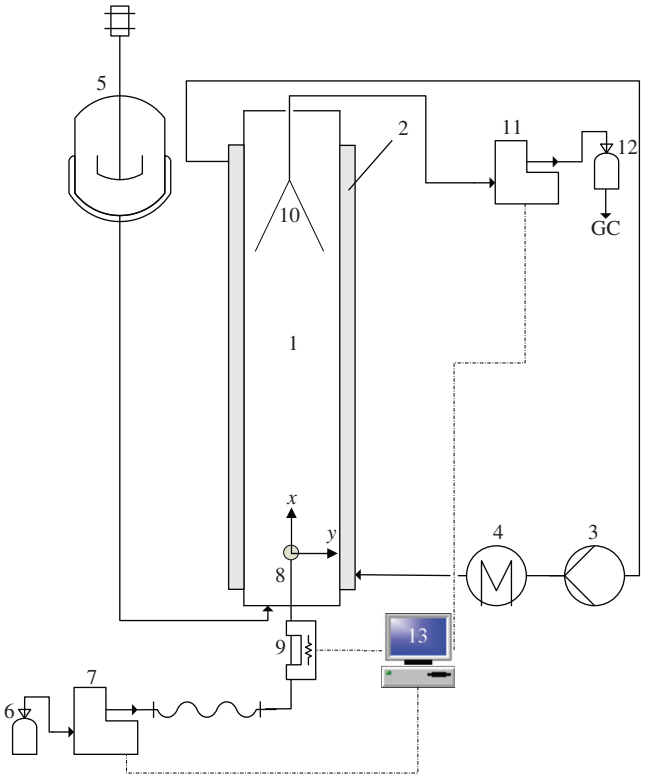

Fig. 2. Experimental setup. (1) Glass column, (2) jacket, (3) thermostat, (4) precision dosing pump, (5) nozzle, (6) solenoid device, (7) saturation tank, (8) high speed camera, (9) illumination system, (10) computer control.

After detachment, the droplet rises in the column and is collected by a funnel device (10). The time interval between two consecutive droplets is large enough (>5 s) so that fluid motion is dampened before the next droplet arrives. The vertical position of the funnel is steplessly variable. The funnel is made of glass with an inner maximum diameter of 70 mm. A small volume of dispersed phase is kept just above the funnel neck in order to allow for drop coalescence at a teflon element. With a second precision dosing pump (11), the dispersed phase is withdrawn dropwise. Only PTFE tubes and fittings were used. Before each measurement, the tube volume is exchanged twice to remove the material created during the last run. Gas chromatography (GC) is used to analyse the dispersed phase sample (12). Thereto, an Agilent 7890 A (with Agilent ChemStation) gas chromatograph was used.

The sample collection procedure is repeated for 10 different contact times for each initial solute concentration. For each contact time, three samples were collected. A mean value is calculated from these three samples. The continuous phase has been changed several times in reasonable intervals to avoid accumulation of solute. Table 3 shows the performed measurements for each mass transfer direction (dispersed to continuous phase $d \rightarrow c$, or vice versa $c \rightarrow d$).

3. Results and discussion

3.1. Comparison with Kronig and Brink model

Fig. 3 shows a comparison of the related mean droplet concentration c^* as a function of time between experimental data and the Kronig and Brink model for different droplet diameters. In the experiments, the mass transfer direction is from the dispersed to the continuous phase and the initial solute concentration is 30 g/L. One can see that the corresponding experimental values for a given diameter are shifted towards the left i.e. that mass transfer is faster than predicted by the model. It should be mentioned that the slope of the model curves is flatter than that of the experimental data. The

Table 2
Physical parameters for $\vartheta = 25$ °C. ρ: density, μ: dynamic viscosity, D_A: diffusion coefficient. Subscript d refers to the dispersed phase, c to the continuous phase and A to the transfer component.

	ρ (kg/m^3)	μ (10^{-4} Pa s)	D_A (10^{-9} m^2/s)
Toluene$_{(d)}$	862.3	5.52	2.9
Water$_{(c)}$	997.02	8.903	1.25
Acetone$_{(A)}$	784.4	3.04	–

Table 3
Experiments performed in the toluene/acetone/water system. c_{Ad0}, $c_{Ac\infty}$: initial solute concentration in the dispersed and continuous phase, respectively.

d_P (mm)	Nozzle	$d \rightarrow c$ c_{Ad0} (g/L) ($c_{Ac\infty} = 0$)				$c \rightarrow d$ $c_{Ac\infty}$ (g/L) ($c_{Ad0} = 0$)		
		0.9	7.5	30	60	1.4	12	49
2.0	N_1	–	–	x	–	–	–	–
3.0	N_1	–	–	x	–	–	–	–
4.0	N_2	–	–	x	–	–	–	–
5.0	N_2	x	x	x	x	x	x	x
6.0	N_3	x	x	x	–	x	x	x
6.9	N_3	x	x	x	–	x	x	–

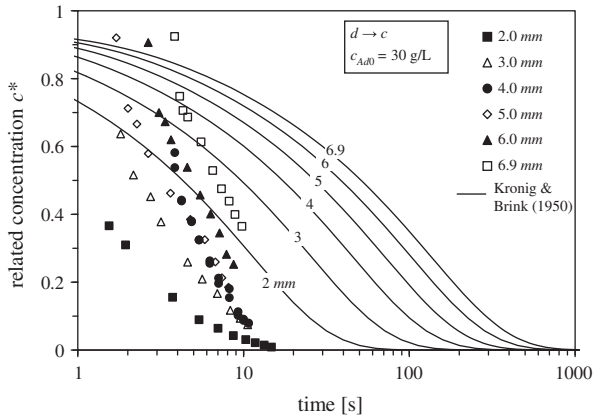

Fig. 3. Related mean droplet concentration c^* as a function of time for different droplet diameters. Comparison between experiments (mass transfer direction $d \rightarrow c$, $c_{Ad0} = 30$ g/L) and Kronig and Brink model.

faster mass transfer is certainly due to Marangoni convection instabilities promoting radial mixing inside the droplet. The Kronig and Brink model does not take into account these effects. The Hadamard streamlines assumed in the model do not exist anymore and were replaced by chaotic convection patterns. Furthermore, for larger droplets, the deformation or oscillation should exhibit an additional effect on the mass transfer rate.

This secondary contribution is estimated in Fig. 4 by applying the following definition of the enhancement factor κ:

$$\kappa = \frac{t_{60,K\&B}}{t_{60,exp}} \tag{8}$$

Here, the enhancement factor is defined as the ratio between the time necessary to complete 60% mass transfer (which is equal to $c^* = 0.4$) predicted by the Kronig and Brink model, $t_{60,K\&B}$, and the time needed in the experiments to achieve the same extraction percentage, $t_{60,exp}$. One can see clearly a bisection in Fig. 4, exactly around the critical diameter d_{cr} where drop oscillation begins, confirmed by experimental observation and predicted by the Klee and Treybal correlation (Klee and Treybal, 1956):

$$d_{cr} = 0.33\rho_c^{-0.14}\Delta\rho^{-0.43}\mu_c^{0.3}\sigma^{0.24} \tag{9}$$

with the density of the continuous phase ρ_c, the density difference between both phases $\Delta\rho$, the dynamic viscosity of the continuous phase μ_c and the interfacial tension σ. Note that the units used in Eq. (9) are the following: $[\rho]$ = g/cm^3, $[\mu] = P$ (Poise), $[\sigma]$ = dyn/cm and $[d_{cr}]$ = cm. For toluene/water, Eq. (9) yields $d_{cr} = 4.45$ mm.

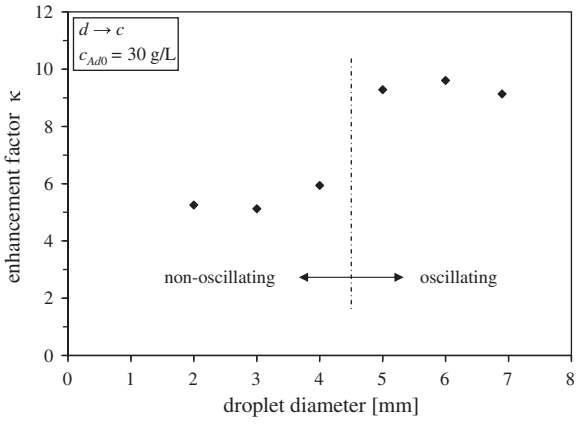

Fig. 4. Enhancement factor κ as a function of droplet diameter.

In the non-oscillating regime, κ is around 5.5, i.e. mass transfer in the Marangoni dominated system is enhanced by this factor compared to the Kronig and Brink prediction. In the oscillating regime, $d_P > d_{cr}$, a distinct step in the κ values can be stated. The enhancement factor is nearly doubled, the mean value is around 9.3. The step indicate a significant change in the relevant mass transfer mechanisms. Beside the Marangoni effects, shape deformations must play a major role with regard to internal mixing behaviour and chaotic convection patterns. The proportion of deformation on the mass transfer enhancement can be estimated by $\kappa_{d_P>d_{cr}}/\kappa_{d_P<d_{cr}}$, thus circa 1.7.

3.2. Comparison with Handlos and Baron model

The influence of the initial solute concentration on the mass transfer as a function of time is shown in Fig. 5 for three different diameters, $d_P = 5.0$ mm (left), $d_P = 6.0$ mm (middle) and $d_P = 6.9$ mm (right). For comparison, the curve predicted by the Handlos and Baron model is plotted in each figure. In the model equations, the reduced droplet velocity has been applied. As mentioned above, Marangoni convection reduces significantly the drop rise velocity, hence the relevant Peclet number to describe the influence of convection compared to the influence of diffusion is reduced as well. The velocities have been determined by measurements comparable to those described in Wegener et al. (2009b). Fifteen sequences have been analysed, and an average value has been calculated. The reproducibility was found to be excellent. It should be noticed, that the Handlos and Baron model (as well as all other models) does not account for the initial solute concentration.

In all three figures, the influence of Marangoni convection on the mass transfer rate is obvious. The higher the initial solute concentration is, the stronger are Marangoni instabilities and the more the curves are shifted to the left, towards faster mass transfer. But compared to the Handlos and Baron model, mass transfer is still slower in the experiments. Even a relatively high concentration of 60 g/L (left figure) cannot be described by the model prediction. Despite the disagreement between experiments and model prediction, the comparison is highly instructive:

- The higher the initial solute concentration is, the nearer are the experimental data to the model curve, i.e. the stronger Marangoni instabilities are, the more the model assumption of turbulent mixing is fulfilled.
- The dynamic of the process i.e. the slope of experimental data is well represented by the Handlos and Baron model, the slope predicted by the Kronig and Brink model was significantly flatter.
- The Handlos and Baron model has no adjustable parameters, but it is the only model which predicts the mean concentration in the Marangoni dominated regime as a function of time, not perfectly, but in the right order of magnitude and relative position.

The influence of droplet diameter on mass transfer as a function of time is shown in Fig. 6 for the three different initial solute concentrations, $c_{Ad0} = 0.9$ g/L (left), $c_{Ad0} = 7.5$ g/L (middle) and $c_{Ad0} = 30$ g/L (right). In all three figures, the mass transfer is the slower the larger the droplet is. This is primarily due to the smaller surface to volume ratio of larger droplets. One should notice that the curves are quasi parallel to one another. Interestingly, the fraction extracted in the drop formation stage is much lower than found in a study recently published by Wegener et al. (2009c) investigating smaller droplet sizes (2.0…4.0 mm). They found extraction rates up to 35% whereas in the present study, the fraction extracted is less than 20%. Primarily, this is due to the larger

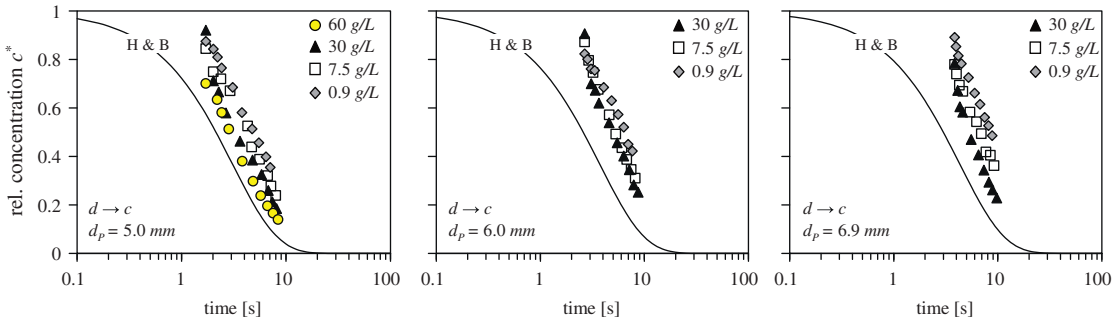

Fig. 5. Related mean droplet concentration c^* as a function of time for different initial solute concentrations. Comparison between experiments ($d \rightarrow c$, $\mu^* = 0.62$, $D_A = 2.9 \times 10^{-9}$ m^2/s) and Handlos and Baron model. Left: $d_P = 5.0$ mm, $v_t = 117$ mm/s, middle: $d_P = 6.0$ mm, $v_t = 116$ mm/s, right: $d_P = 6.9$ mm, $v_t = 115$ mm/s.

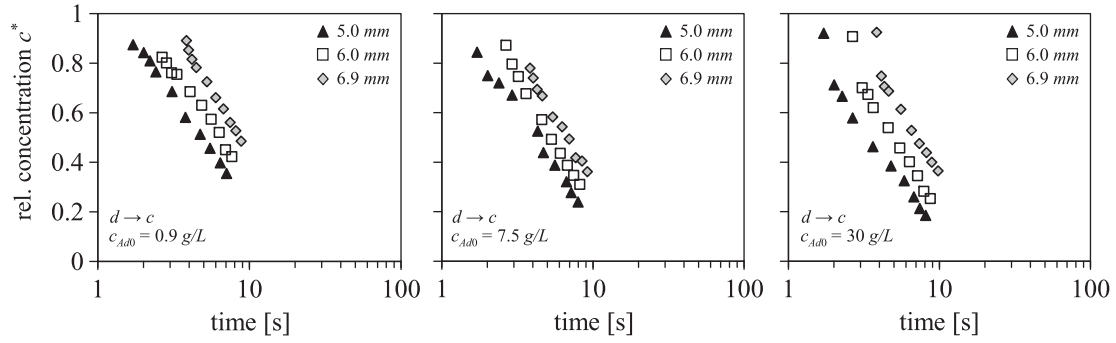

Fig. 6. Related mean droplet concentration c^* as a function of time for different drop diameters ($d \rightarrow c$). Left: $c_{Ad0} = 0.9$ g/L, middle: $c_{Ad0} = 7.5$ g/L, right: $c_{Ad0} = 30$ g/L.

nozzle diameter used in the present investigations leading to a lower nozzle Reynolds number and thus less convection driven mass transfer compared to a smaller nozzle.

In spherical droplets with laminar circulation of Hadamard type assumed in the Kronig and Brink model ($Re < 1$, $Pe \rightarrow \infty$), mass transfer is due to diffusion perpendicular to the isolines of concentration, a convective radial mixing is not considered. In the Kronig and Brink model, time of diffusion increases with the square of droplet diameter. In consequence, the related mean droplet concentration c^* can be expressed with one single curve for different droplet diameters if c^* is plotted versus the Fourier number $Fo = 4tD_A/d_P^2$. Regardless of droplet size, the model reflects the fact that the relevant transport mechanisms are identical for all diameters.

Although in processes with Marangoni instabilities, convection is dominant over diffusion, the experimental data of Fig. 6 are plotted as a function of Fourier number in Fig. 7. The result shows that in this plot the experimental data for different diameters fall into one single curve, independent of the used initial solute concentration. One might guess from this result that mass transfer in oscillating droplets with simultaneous Marangoni convection scales with the square of droplet diameter and the relative position of the c^*-curve depends on the initial solute concentration.

This result simplifies the modelling approach, as exemplarily shown in Fig. 8. Since the data of all three diameters of one initial solute concentration fall into one single curve, the Handlos and Baron model can be used to express the experimental data. Only a slight modification is introduced, namely a single concentration dependent parameter $\alpha(\Delta c_{A,0})$, to reflect the influence of the initial solute concentration difference between both phases:

$$c^* = exp\left[-\alpha(\Delta c_{A,0})\frac{\lambda_n\, v_t\, t}{128\, d_P\,(1+\mu^*)}\right] \tag{10}$$

For all three figures, the reduced rise velocity of a 5 mm-droplet ($v_t = 117$ mm/s) is used. The modification parameter α increases with increasing initial solute concentration, see Table 4. The agreement

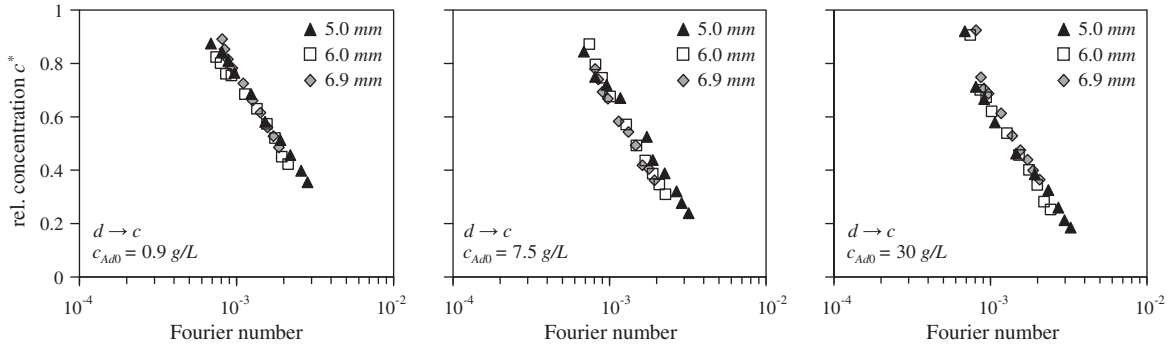

Fig. 7. Related mean droplet concentration c^* as a function of Fourier number for different drop diameters ($d \rightarrow c$). Left: $c_{Ad0} = 0.9$ g/L, middle: $c_{Ad0} = 7.5$ g/L, right: $c_{Ad0} = 30$ g/L.

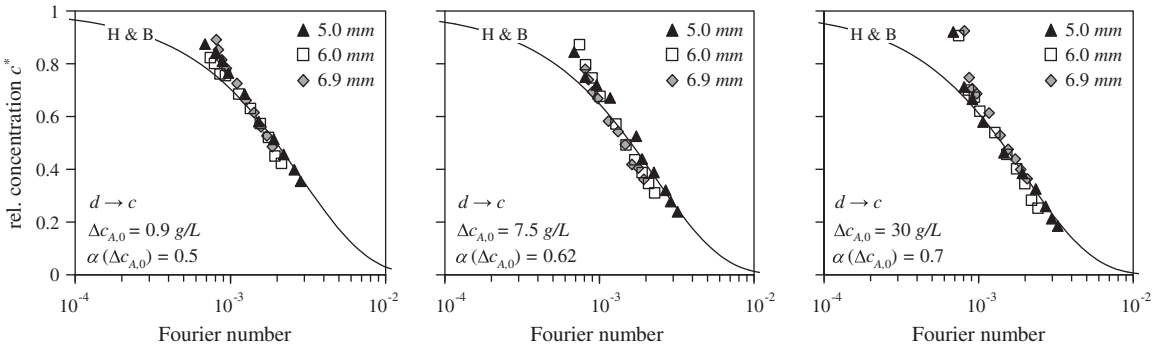

Fig. 8. Related mean droplet concentration c^* as a function of Fourier number for different drop diameters ($d \rightarrow c$) compared to the modified Handlos and Baron model. Left: $c_{A,0}$ = 0.9 g/L, α = 0.5, middle: $c_{A,0}$ = 7.5 g/L, α = 0.62, right: $c_{A,0}$ = 30 g/L, α = 0.7. Global parameters for the modified model: d_P = 5 mm, v_t = 117 mm/s, λ_n = 2.88, $1 + \mu^*$ = 1.62.

between the modified Handlos and Baron model with the experimental data is satisfying. Fig. 9 shows a parity plot of calculated and experimental data. The majority of the data lies within a tolerance of ±20%. The deviation becomes more significant for short times, i.e. when drop formation is over and free rise begins which is not surprising since the phenomena during drop formation are complex and not well understood (see e.g. Wegener et al., 2009c).

Finally, the influence of the mass transfer direction has been investigated. The solute concentration in the droplet phase is zero at the beginning, the initial solute concentrations in the continuous phase are 1.4, 12 and 49 g/L, see Table 3. The ratio of the initial solute concentrations for both transfer directions is equal to the distribution coefficient m (Wegener et al., 2009c):

Table 4
Modification parameter α as a function of initial solute concentration difference $\Delta c_{A,0}$.

$\Delta c_{A,0}$ (g/L)	0.9	7.5	30
α	0.5	0.62	0.7

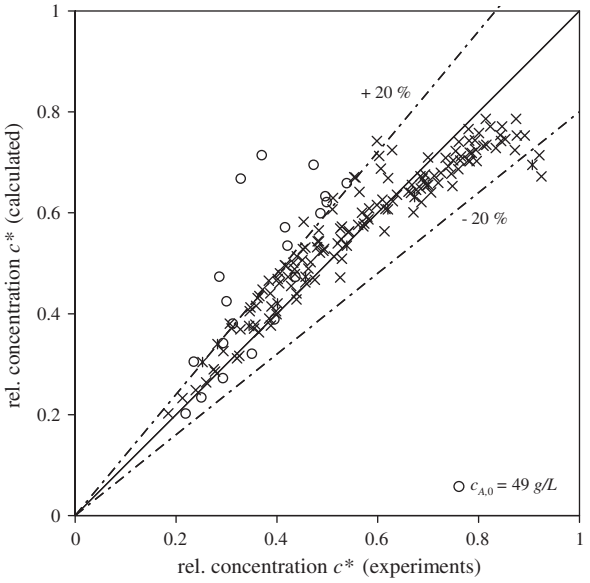

Fig. 9. Parity plot of all experimental data (both mass transfer directions, diameters 5, 6 and 6.9 mm and initial concentrations as shown in Table 3) compared with model prediction (modified Handlos and Baron model) for the related mean droplet concentration c^*. The circles indicate the case $c \rightarrow d$ with $c_{A,0}$ = 49 g/L, d_P = 5 and 6 mm (system with hindered coalescence).

$$\frac{c_{A,0(d\rightarrow c)}}{c_{A,0(c\rightarrow d)}} = m \tag{11}$$

With Eq. (11), the maximum amount of solute to be transported is equal in both cases. According to earlier works (e.g. Wegener et al., 2009c), m is set to 0.63. Fig. 10 shows the result in comparison with the modified Handlos and Baron model using the same α values displayed in Table 4 for the corresponding initial solute concentration for the opposite mass transfer direction according to Eq. (11). For the lower initial solute concentration, all data points coincide with one curve, well represented by the model equation. This shows that mass transfer enhancement due to Marangoni convection is comparable to the reversed mass transfer direction. For $c_{A,0}$ = 12 g/L, the slope of the experimental data becomes flatter and the agreement with the model is less satisfying, but predominantly ±20%. The data are also displayed in the parity plot, Fig. 9.

The worst result is shown in Fig. 10, right ($c_{A,0}$ = 49 g/L). In Fig. 9, these data are represented by open circles and show deviations up to 100%. On one hand, the self similarity seems to be unvalid, the scattering of data is enormous. 6.9 mm droplets could not have been realized since the droplets detached from the nozzle tip before drop formation was over due to strong lateral drop motion caused by Marangoni convection. The unsatisfying agreement between model and experimental data can be explained with the hindered coalescence in the funnel device. In the mass transfer direction $c \rightarrow d$, Marangoni effects hinder drop coalescence, as observed e.g. by Chevaillier et al. (2006), Hoting (1996), Reissinger and Marr (1986). This causes problems due to a random coalescence time and thus unreproducable residence time of the droplets until they are withdrawn by the pump. In this case, the end effect "coalescence" dominates the mass transfer at the end of the free rise stage and makes comparison difficult. Thus, further investigations are necessary on this issue to examine the influence of coalescence probability on extraction efficiency.

4. Conclusions

An in-depth study on the influence of Marangoni convection on the mass transfer at deformable single rising droplets has been carried out in the standard test system toluene/acetone/water. Parameters varied were the droplet diameter, the initial solute concentration and the mass transfer direction. Comparisons with mass transfer models from literature, especially Kronig and Brink (1950) and Handlos and Baron (1957) lead to the following conclusions:

- Mass transfer in Marangoni dominated systems cannot be described by the Kronig and Brink model which assumes laminar circulation of Hadamard type inside the droplet. Marangoni

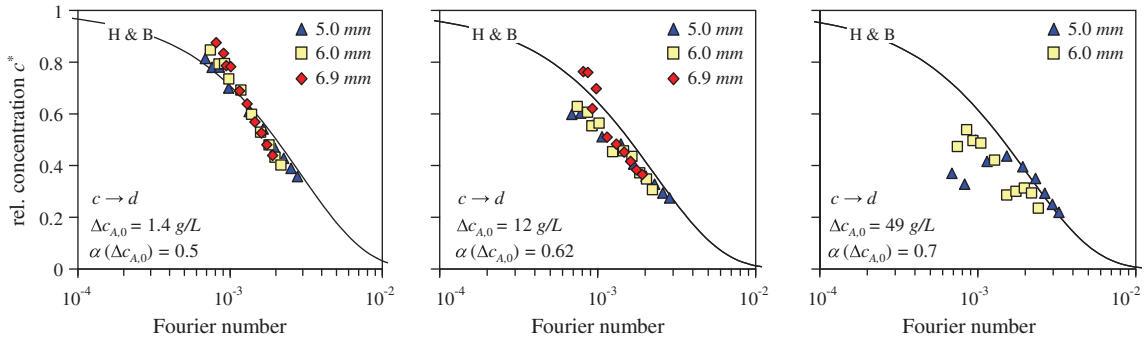

Fig. 10. Related mean droplet concentration c^* as a function of Fourier number for different drop diameters for the reversed mass transfer direction ($c \rightarrow d$) compared to the modified Handlos and Baron model. Left: $c_{A,0}$ = 1.4 g/L, α = 0.5, middle: $c_{A,0}$ = 12 g/L, α = 0.62, right: $c_{A,0}$ = 49 g/L, α = 0.7. Global parameters for the modified model: d_P = 5 mm, v_t = 117 mm/s, λ_n = 2.88,1 + μ^* = 1.62.

convection destroys these laminar circulation patterns, instead, chaotic convection leads to enhanced radial mixing and thus higher mass transfer rates.

- The enhancement factor based on the Kronig and Brink model indicates that mass transfer is more than five times higher in the toluene/acetone/water system when droplet shape is spherical. In the oscillating regime, a distinct step in the enhancement factor occurs, the mass transfer is enhanced by a factor of nearly 2 compared to the non-oscillating regime which reflects the contribution of droplet deformation.
- The original Handlos and Baron model cannot describe the influence of Marangoni convection properly, since it does not account for the effect of initial solute concentration on the strength of Marangoni convection. But it seems that, at least for the system toluene/acetone/water, the Handlos and Baron model represents the state of turbulent perfect mixing. The experimental data approach the model curve if Marangoni convection is strong. The slope of the model curve is comparable to most of the experimental data.
- The experimental data fall on one curve if the values for the different droplet diameters are plotted against the Fourier number. Apparently, the mass transfer scales with the square of the droplet diameter. This finding has been approved for all initial solute concentrations and both mass transfer directions, but not for the case when coalescence is hindered ($c \rightarrow d$, $c_{A,0}$ = 49 g/L).
- A single parameter α is introduced to modify the Handlos and Baron model. It accounts for the influence of the initial solute concentration on the mass transfer. α is fitted to experimental data and leads to excellent agreement. Only for short times, reflecting the influence of the complex process of droplet formation, the agreement is less pronounced.

Special care was taken in order to keep the system free of surfactants or contaminants. In many industrial applications, surfactants play a significant role in the mass transfer process. The objective of future work will be to extend our existing works on Marangoni effects in clean single droplet systems to a controlled contamination with surfactants. The complex interaction of Marangoni effects, droplet deformation and the presence of surfactants will be investigated.

Acknowledgement

The authors like to thank the German Research Foundation (DFG) for financial support.

References

Agble, D., Mendes-Tatsis, M.A., 2000. The effect of surfactants on interfacial mass transfer in binary liquid–liquid systems. Int. J. Heat Mass Transfer 43, 1025–1034.
Al-Hassan, T., Mumford, C.J., Jeffreys, G.V., 1992. A study of mass transfer from single large oscillating drops. Chem. Eng. Technol. 15, 186–192.
Angelo, J.B., Lightfoot, E.N., Howard, D.W., 1966. Generalization of the penetration theory for surface stretch: application to forming and oscillating drops. AIChE J. 12, 751–760.
Calderbank, P.H., Korchinski, I.J.O., 1956. Circulation in liquid drops: (a heat-transfer study). Chem. Eng. Sci. 6, 65–78.
Chevaillier, J.P., Klaseboer, E., Masbernat, O., Gourdon, C., 2006. Effect of mass transfer on the film drainage between colliding drops. J. Colloid Interface Sci. 299, 472–485.
Clift, R., Grace, J.R., Weber, M.E., 1978. Bubbles, Drops, and Particles. Academic Press, New York.
Handlos, A.E., Baron, T., 1957. Mass and heat transfer from drops in liquid–liquid extraction. AIChE J. 3, 127–136.
Hoting, B., 1996. Untersuchungen zur Fluiddynamik und Stoffbertragung in Extraktionskolonnen mit strukturierten Packungen. Fortschrittberichte VDI Reihe 3 Number 439.
Hubis, M., Hartland, S., 1986. Limitations of the Handlos–Baron model. Chem. Eng. Sci. 41, 2436–2437.
Henschke, M., Pfennig, A., 1999. Mass-transfer enhancement in single-drop extraction experiments. AIChE J. 45, 2079–2086.
Klee, A.J., Treybal, R.E., 1956. Rate of rise or fall of liquid drops. AIChE J. 2, 444–447.
Kronig, R., Brink, J.C., 1950. On the theory of extraction from falling droplets. Appl. Sci. Res. Sec. a – Mech. Heat Chem. Eng. Math. Methods 2, 142–154.
Loth, E., 2008. Quasi-steady shape and drag of deformable bubbles and drops. Int. J. Multiphase Flow 34, 523–546.
Magarvey, R.H., Kalejs, J., 1963. Internal circulations within liquid drops. Nature 198, 377–378.
Mao, Z.-S., Chen, J., 2004. Numerical simulation of the Marangoni effect on mass transfer to single slowly moving drops in the liquid–liquid system. Chem. Eng. Sci. 59, 1815–1828.
Mekasut, L., Molinier, J., Angelino, H., 1979. Effects of surface-active agents on mass transfer inside drops. Chem. Eng. Sci. 34, 217–224.
Misek, T., Berger, R., Schröter, J., 1985. Standard test systems for liquid extraction. Inst. Chem. Eng., EFCE Publ. Series, 46.
Newman, A.B., 1931. The drying of porous solid. Diffusion and surface emission effects. Trans. AIChE 27, 203–216.
Olander, D.R., 1966. Handlos–Baron drop extraction model. AIChE J. 12, 1018–1019.
Petera, J., Weatherley, L.R., 2001. Modelling of mass transfer from falling droplets. Chem. Eng. Sci. 56, 4929–4947.
Reissinger, K.-H., Marr, R., 1986. Auslegungskonzept für pulsierte Siebboden-Extraktoren. Chem. Ing. Technik 58, 540–547.
Rose, P.M., Kintner, R.C., 1966. Mass transfer from large oscillating drops. AIChE J. 12, 530–534.
Schulze, K., 2007. Stoffaustausch und Fluiddynamik am bewegten Einzeltropfen unter dem Einfluss von Marangonikonvektion. PhD thesis, Chair of Chemical & Process Engineering, TU Berlin, Germany. URL: <http://opus.kobv.de/tuberlin/volltexte/2007/1672/>.
Slater, M.J., 1994. Rate coefficients in liquid–liquid extraction systems. In: Godfrey, J.C., Slater, M.J. (Eds.), Liquid–Liquid Extraction Equipment. John Wiley & Sons Ltd., Baffins Lane, Chichester, England.
Spells, K.E., 1952. A study of circulation patterns within liquid drops moving through a liquid. Proc. Phys. Soc. Sect. B 65, 541.
Sternling, C.V., Scriven, L.E., 1959. Interfacial turbulence: hydrodynamic instability and the Marangoni effect. AIChE J. 5, 514–523.

Wegener, M., Grünig, J., Stüber, J., Paschedag, A.R., Kraume, M., 2007. Transient rise velocity and mass transfer of a single drop with interfacial instabilities – experimental investigations. Chem. Eng. Sci. 62, 2967–2978.

Wegener, M., Eppinger, T., Bäumler, K., Kraume, M., Paschedag, A.R., Bänsch, E., 2009a. Transient rise velocity and mass transfer of a single drop with interfacial instabilities – numerical investigations. Chem. Eng. Sci. 64, 4835–4845.

Wegener, M., Fevre, M., Paschedag, A.R., Kraume, M., 2009b. Impact of Marangoni instabilities on the fluid dynamic behaviour of organic droplets. Int. J. Heat Mass Transfer 52, 2543–2551.

Wegener, M., Paschedag, A.R., Kraume, M., 2009c. Mass transfer enhancement through Marangoni instabilities during single drop formation. Int. J. Heat Mass Transfer 52, 2673–2677.

Wegener, M., Kraume, M., Paschedag, A.R., 2010. Terminal and transient drop rise velocity of single toluene droplets in water. AIChE J. 56, 2–10.

Yamaguchi, M., Watanabe, S., Katayama, T., 1975. Experimental studies on mass transfer rate around single oscillating drops in liquid–liquid systems. J. Chem. Eng. Jpn. 8, 415–417.